ARTICLES

Uphill Photooxidation of NADH Analogues by Hexyl Viologen Catalyzed by Zinc Porphyrin-Linked Fullerenes†

Shunichi Fukuzumi,*,‡ Hiroshi Imahori,*,‡ Ken Okamoto,‡ Hiroko Yamada,‡ Mamoru Fujitsuka,§ Osamu Ito,*,§ and Dirk M. Guldi*,||

Department of Material and Life Science, Graduate School of Engineering, Osaka University, CREST, Japan Science and Technology Corporation (JST), Suita, Osaka 565-0871, Japan, and Institute of Multidisciplinary Research for Advanced Materials, Tohoku University, CREST, Japan Science and Technology Corporation (JST), Sendai, Miyagi 980-8577, Japan, and Radiation Laboratory, University of Notre Dame, Notre Dame, Indiana 46556

Received: April 27, 2001; In Final Form: June 27, 2001

In the absence of oxygen, the photolytically generated $C_{60}^{\bullet-}$ moiety in $ZnP^{\bullet+}-C_{60}^{\bullet-}$ and $ZnP^{\bullet+}-H_2P-C_{60}^{\bullet-}$ radical ion pairs undergoes one-electron oxidation by hexyl viologen (HV^{2+}), whereas the $ZnP^{\bullet+}$ moiety is reduced by NADH analogues (1-benzyl-1,4-dihydronicotinamide and 10-methyl-9,10-dihydroacridine). Thus, both $ZnP-C_{60}$ and $ZnP-H_2P-C_{60}$ donor−acceptor ensembles act in benzonitrile as efficient photocatalysts for the uphill oxidation of NADH analogues by HV^{2+}. In the case of $ZnP-C_{60}$, the quantum yield of the photocatalytic reaction increases with increasing concentration of HV^{2+} or an NADH analogue to reach a limiting value of 0.99. The limiting quantum yields of $ZnP-C_{60}$ and $ZnP-H_2P-C_{60}$ agree well with the quantum yields of radical ion pair formation, $ZnP^{\bullet+}-C_{60}^{\bullet-}$ and $ZnP^{\bullet+}-H_2P-C_{60}^{\bullet-}$, respectively. In the presence of oxygen, the lifetimes of the radical ion pairs are, however, markedly reduced because of an oxygen-catalyzed back electron transfer process between $C_{60}^{\bullet-}$ and $ZnP^{\bullet+}$. Such an impact on the radical ion pair lifetime consequences a significant decrease in the photocatalytic reactivity of the dyad (i.e., $ZnP-C_{60}$) in the overall photooxidation of an NADH analogue by HV^{2+}. By contrast, the reactivity of the triad (i.e., $ZnP-H_2P-C_{60}$) shows little effects upon admitting O_2.

Introduction

The spherical shape of C_{60}, containing sixty delocalized π electrons, renders these carbon allotropes ideal components for the construction of efficient electron transfer model systems. Most importantly, the small reorganization energy, found for C_{60} in electron transfer processes, results, on one hand, in an overall acceleration of the charge separation (CS) step, whereas on the other hand, a deceleration was noted for the energy-wasting charge recombination (CR) step.[1−3] Thus, efficient stepwise CS, for example, in fullerene-based dyad, triad, and tetrad ensembles, has been accomplished along well-designed and fine-tuned redox gradients.[1−3] The resulting high-energy CS state is converted into electrical energy by constructing integrated artificial photosynthetic assemblies on gold electrodes with the use of self-assembled monolayers (SAMs).[4,5] However, the conversion of the high-energy CS state in fullerene-containing donor−acceptor linked systems into chemical energy has yet to be reported, although there have been some reports on uphill photochemical reactions catalyzed by other photosensitizers.[6−8]

In the biological redox systems, the $NADH/NAD^+$ system (NAD^+ = nicotinamide adenine dinuclotide; NADH = reduced form of NAD^+) plays a key role in energy conversion and storage.[9−11] In fact, NADH is a source of two electrons and a proton, which is the equivalent to a hydride ion.[9−11] Once NADH is oxidized to NAD^+, it is, however, rather difficult to reduce NAD^+ back to NADH by a one-electron reducing entity. The intrinsic stability of NAD^+ relates to its low reduction potential (−1.1 V vs. SCE) although the overall two-electron process is thermodynamically favorable.[10,11] An NADH analogue, 9-phenyl-10-methyl-9,10-dihydroacridine (AcrHPh) has previously been used as an electron source in the direct photochemical oxidation of AcrHPh by *N*,*N*'-dimethyl-4,4'-bipyridinium dication (methyl viologen, MV^{2+}) without a photocatalyst.[12] The amount of energy stored in this photochemical oxidation was estimated as 0.76 eV (73 kJ mol^{-1}).[12]

In this study, we wish to report on highly efficient energy conversion systems, based on several C_{60}-containing donor acceptor ensembles, zinc porphyrin−C_{60} ($ZnP-C_{60}$) and zinc porphyrin−free base porphyrin−fullerene triad ($ZnP-H_2P-C_{60}$). These systems act as novel photocatalysts for the uphill oxidation of NADH analogues by hexyl viologen (HV^{2+}) in the absence of oxygen. By contrast, upon admitting oxygen, the rate limiting back electron transfer (BET) process, that is, CR between the fullerene radical anion and the zinc porphyrin radical cation, was accelerated profoundly without forming

† Part of the special issue "Noboru Mataga Festschrift".

* To whom correspondence should be addressed. E-mail: fukuzumi@ap.chem.eng.osaka-u.ac.jp. E-mail: imahori@ap.chem.eng.osaka-u.ac.jp. E-mail: ito@tagen.tohoku.ac.jp. E-mail: guldi.1@nd.edu.

‡ Osaka University.

§ Tohoku University.

|| University of Notre Dame.

10.1021/jp011613g CCC: $22.00
Published on Web 08/04/2001

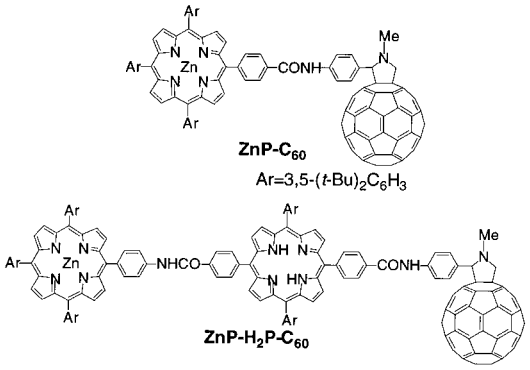

Figure 1. Structures of ZnP−C_{60} and ZnP−H_2P−C_{60}.

reactive oxygen species, such as singlet oxygen or superoxide anion.[13] The effects of O_2 on the photocatalytic reactivity of ZnP−C_{60} and ZnP−H_2P−C_{60} are also examined in relation with the catalytic effects of O_2 on the BET reactions.[13]

Experimental Section

Materials. The synthesis and characterization of the porphyrin-fullerene linked molecules (ZnP−C_{60}[3,14] and ZnP−H_2P−C_{60}[3]) have been described previously (see Figure 1). Preparation of 1-benzyl-1,4-dihydronicotinamide (BNAH) and the BNA dimer was described previously.[15] 10-Methyl-9,10-dihydroacridine ($AcrH_2$) was prepared from 10-methylacridinium iodide ($AcrH^+I^-$) by the reduction with $NaBH_4$ in methanol and purified by recrystallization from ethanol.[15] $AcrH^+I^-$ was prepared by the reaction of acridine with methyl iodide in acetone and was converted to the perchlorate salt ($AcrH^+ClO_4^-$) by the addition of magnesium perchlorate to the iodide salt ($AcrH^+I^-$) and purified by recrystallization from methanol.[16] Tetrabutylammonium hexafluorophosphate used as a supporting electrolyte for the electrochemical measurements was obtained from Tokyo Kasei Organic Chemicals. Benzonitrile was purchased from Wako Pure Chemical Ind., Ltd. and purified by successive distillation over calcium hydride. The synthesized 1,1-dihexyl-4,4'-dipyridinium dibromide and the corresponding diperchlorate salt (HV^{2+}) were described previously.[13,17]

Quantum Yield Determinations. A standard actinometer (potassium ferrioxalate)[18] was used for the quantum yield determination of the photochemical reactions of NADH analogues with hexyl viologen in the presence of ZnP−C_{60} or ZnP−H_2P−C_{60}. Typically, a square quartz cuvette (10 mm i.d.) which contained a deaerated PhCN solution (3.0 cm^3) of ZnP−C_{60} (3.0×10^{-6} M), BNAH (4.0×10^{-4} M), and HV^{2+} (8.0×10^{-4} M) was irradiated with monochromatized light of $\lambda = 433$ nm from a Shimadzu RF-5000 fluorescence spectrophotometer. Under the conditions of actinometry experiments, the actinometer and ZnP−C_{60} absorbed essentially all of the incident light of $\lambda = 433$ nm. The light intensity of monochromatized light of $\lambda = 433$ nm was determined as 9.22×10^{-9} einstein s^{-1} with the slit width of 20 nm. The photochemical reaction was monitored using a Hewlett Packard 8452A diode-array spectrophotometer. The quantum yields in the absence of oxygen were determined from increase in absorbance of $HV^{\bullet+}$ at 615 nm ($\epsilon = 10\,000$ M^{-1} cm^{-1}). The ϵ value was determined by the quantitative reduction of HV^{2+} by tetramethylsemiquinone radical anion which was prepared by the dispoportionation reaction of tetramethylhydroquinone and the dianion obtained by deprotonation with tetrabutylammonium hydroxide.[19] In the presence of oxygen, the quantum yields of the photooxidation of $AcrH_2$ by HV^{2+} were determined from increase in absorbance of $AcrH^+$ at 358 nm ($\epsilon = 18\,000$ M^{-1} cm^{-1}).[20] In order to avoid the contribution of light absorption of the products, only the initial rates were used for determination of the quantum yields.

SCHEME 1

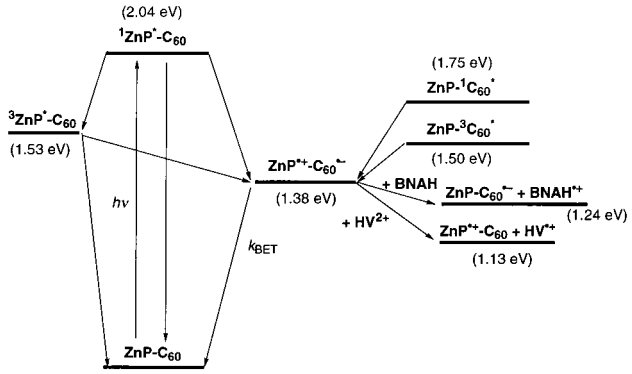

Laser Flash Photolysis. Nanosecond transient absorption measurements were carried out using SHG (532 nm) of a Nd:YAG laser (Spectra-Physics, Quanta-Ray GCR-130, fwhm 6 ns) as an excitation source. For transient absorption spectra in the near-IR region (600−1600 nm), monitoring light from a pulsed Xe lamp was detected with a Ge-avalanche photodiode (Hamamatsu Photonics, B2834). Photoinduced events in micro- and millisecond time regions were estimated by using a continuous Xe lamp (150 W) and an InGaAs-PIN photodiode (Hamamatsu Photonics, G5125-10) as a probe light and a detector, respectively. Details of the transient absorption measurements were described elsewhere.[3] All of the samples in a quartz cell (1 × 1 cm) were deaerated by bubbling argon through the solution for 15 min.

Electrochemical Measurements. The cyclic voltammetry (CV) measurements were performed on a BAS 50 W electrochemical analyzer in a deoxygenated PhCN solution containing 0.10 M *n*-Bu_4NPF_6 as a supporting electrolyte at 298 K. The differential pulse voltammetry measurements were also performed on a BAS 50 W electrochemical analyzer in a deaerated PhCN solution containing 0.10 M *n*-Bu_4NPF_6 as a supporting electrolyte at 298 K (10 mV s^{-1}). The glassy carbon working electrode was polished with BAS polishing alumina suspension and rinsed with acetone before use. The counter electrode was a platinum wire. The measured potentials were recorded with respect to an Ag/AgCl (saturated KCl) reference electrode. Ferrocene/ferricenium was used as an external standard.

Results and Discussion

Photocatalytic Oxidation of BNAH by HV^{2+}. The energy levels of the singlet and triplet excited states of the investigated ZnP−C_{60} dyad in PhCN are summarized in Scheme 1, illustrating the different relaxation pathways following the initial photoexcitation event of ZnP−C_{60}.[3] Time-resolved techniques, including fluorescence lifetime and transient absorption measurements, have been employed to probe the CS and CR dynamics in this donor-acceptor array, disclosing the formation of the $ZnP^{\bullet+}-C_{60}^{\bullet-}$ pair in a variety of solvents.[3,13] With the help of these time-resolved studies we determined the quantum yield of the radical ion pair formation as $\Phi_1 = 0.99$.[3] The rate of intramolecular back electron transfer (k_{BET}) from $C_{60}^{\bullet-}$ to $ZnP^{\bullet+}$ in $ZnP^{\bullet+}-C_{60}^{\bullet-}$, is 1.3×10^6 s^{-1} in oxygen-free PhCN solutions.[3]

The photophysics of the second compound, namely, ZnP−H_2P−C_{60}, in PhCN are well-studied.[3] An initial singlet−singlet energy transfer from the $^1ZnP^*$ moiety (2.04 eV) to the H_2P

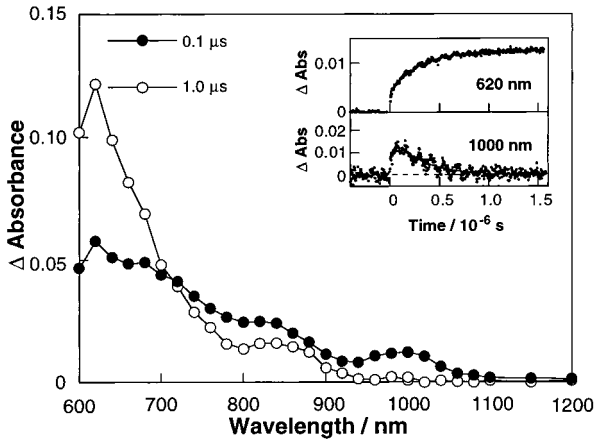

Figure 2. Transient absorption spectra of a PhCN solution containing ZnP−C_{60} (1.0×10^{-4} M) and HV^{2+} (3.5×10^{-3} M) after laser excitation (0.1 and 1 μs) in deaerated PhCN. Inset: Absorption-time profiles at 620 and 1000 nm.

moiety (1.89 eV) is followed by a sequential ET relay starting with the ZnP−$^1H_2P^*$−C_{60} via the transient ZnP−$H_2P^{\bullet+}$−$C_{60}^{\bullet-}$ (1.63 eV) to yield finally the $ZnP^{\bullet+}$−H_2P−$C_{60}^{\bullet-}$ (1.34 eV). The individual charge shift reactions are, however, in competition with the back ET to the ground state and triplet excited states, resulting in only a moderate quantum yield (0.40) for the final radical ion pair formation ($ZnP^{\bullet+}$−H_2P−$C_{60}^{\bullet-}$).[3] On the other hand, the large distance, separating the donor and acceptor moieties, is beneficial with respect to increasing the lifetime ($k_{BET} = 4.8 \times 10^4\ s^{-1}$) of the $ZnP^{\bullet+}$−H_2P−$C_{60}^{\bullet-}$ pair by a factor of 27 relative to that noted for the ZnP$^{\bullet+}$−$C_{60}^{\bullet-}$ pair.[3,13]

A comparison between the one-electron oxidation potential of $C_{60}^{\bullet-}$ (E^0_{ox} = -0.67 V vs SCE, which is equivalent to the one-electron reduction potential of C_{60}) and the one-electron reduction potential of HV^{2+} (E^0_{red} = -0.42 V vs SCE) unravels that an electron transfer from $C_{60}^{\bullet-}$ to HV^{2+} is exergonic by 0.25 eV (Scheme 1). In fact, when HV^{2+} is added to the ZnP−C_{60} system, a direct electron transfer from $C_{60}^{\bullet-}$ in the radical ion pair ($ZnP^{\bullet+}$−$C_{60}^{\bullet-}$) to HV^{2+} occurs, producing $HV^{\bullet+}$ (λ_{max} = 615 nm) as shown in Figure 2. Importantly, the decay of the $C_{60}^{\bullet-}$ absorption at 1000 nm[21] coincides with the appearance of $HV^{\bullet+}$ at 615 nm (see inset of Figure 2), and furthermore, the decay rate varies linearly with HV^{2+} concentration. These findings serve as crucial testimony for the existence of a one-electron transfer between the photolytically generated $C_{60}^{\bullet-}$ (i.e., $ZnP^{\bullet+}$−$C_{60}^{\bullet-}$) and HV^{2+} to form the stable $HV^{\bullet+}$.

The transient features of $ZnP^{\bullet+}$ are not affected by this reaction and remain virtually stable on the monitored time scale shown in Figure 2.[13] The second-order rate constant of the intermolecular electron transfer is determined from the formation rate of $HV^{\bullet+}$ as $(7 \pm 2) \times 10^8\ M^{-1}\ s^{-1}$. Thus, the rate of intermolecular electron transfer from $C_{60}^{\bullet-}$ to HV^{2+} ($2.5 \times 10^6\ s^{-1}$ at 3.5×10^{-3} M of HV^{2+}) competes well with the rate of intramolecular back electron transfer from $C_{60}^{\bullet-}$ to $ZnP^{\bullet+}$ in $ZnP^{\bullet+}$−$C_{60}^{\bullet-}$ ($k_{BET} = 1.3 \times 10^6\ s^{-1}$).[3]

If $ZnP^{\bullet+}$ is indeed reduced by an external electron donor such as BNAH, separately added to the ZnP−C_{60}/HV^{2+} or ZnP−H_2P−C_{60}/HV^{2+} systems, ZnP−C_{60} or ZnP−H_2P−C_{60} may, in fact, photocatalyze the overall oxidation of BNAH by HV^{2+} (Scheme 2). An electron transfer from BNAH to $ZnP^{\bullet+}$ is expected to be exothermic, considering the one-electron oxidation potential of BNAH (E^0_{ox} = 0.57 V vs SCE),[15] which is 0.14 V less positive than the one-electron reduction potential of $ZnP^{\bullet+}$ (0.71 V vs SCE, which is equivalent to the one-electron oxidation potential of ZnP).[13] Thus, once the CS state is obtained

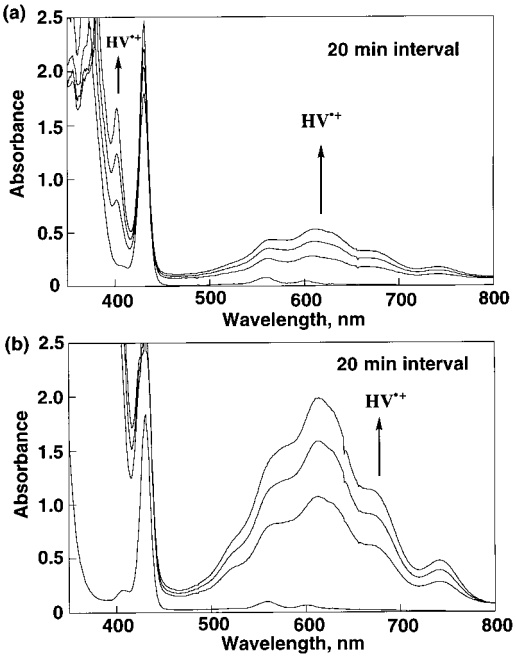

Figure 3. (a) Spectral change observed in the steady-state photolysis of a PhCN solution of BNAH (4.0×10^{-4} M), HV^{2+} (8.0×10^{-4} M), and ZnP−C_{60} (3.0×10^{-6} M) under irradiation with monochromatized light of λ = 433 nm. (b) Spectral change observed in the steady-state photolysis of a PhCN solution of BNAH (4.0×10^{-4} M), HV^{2+} (8.0×10^{-4} M), and ZnP−H_2P−C_{60} (3.0×10^{-6} M) under irradiation with monochromatized light of λ = 433 nm.

SCHEME 2

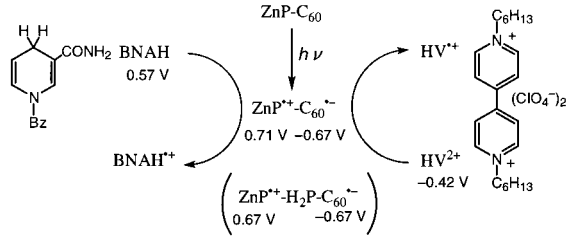

via photoirradiation of ZnP−C_{60} or ZnP−H_2P−C_{60}, the oxidation of BNAH and the reduction of HV^{2+} should be accomplished by a reaction with $ZnP^{\bullet+}$ and $C_{60}^{\bullet-}$, respectively (Scheme 2).[22] Hereby, the longer lifetime of the $ZnP^{\bullet+}$−spacer−$C_{60}^{\bullet-}$ state in the triad as compared to that in the dyad (vide supra) may result in facilitated redox reactions involving the CS state, BNAH and HV^{2+}.

In fact, this pathway was experimentally confirmed by photolysis of the ZnP−C_{60}/BNAH/HV^{2+} and ZnP−H_2P−C_{60}/BNAH/HV^{2+} systems with visible light (433 nm) in deoxygenated PhCN. For instance, Figure 3a,b depicts the steady state photolysis in deoxygenated PhCN, in which the $HV^{\bullet+}$ absorption band (λ_{max} = 402 and 615 nm) increases progressively with irradiation time. By contrast, no reaction occurs in the dark or in the absence of the photocatalyst (i.e., ZnP−C_{60} or ZnP−H_2P−C_{60}) under photoirradiation. Once $HV^{\bullet+}$ is generated in the photochemical reaction, it was found to be stable in deoxygenated PhCN. The stoichiometry of the reaction is established by employing eq 1,

$$\mathrm{BNAH} + 2\mathrm{HV}^{2+} \xrightarrow[\substack{\mathrm{ZnP-C_{60}}\\ \mathrm{ZnP-H_2P-C_{60}}}]{h\nu} \mathrm{BNA}^{+} + 2\mathrm{HV}^{\bullet+} + \mathrm{H}^{+} \quad (1)$$

where BNAH acts as a two-electron donor to reduce two equivalents of $HV^{\bullet+}$.

TABLE 1: Quantum Yields (Φ_{obs}) of Photocatalytic Oxidation of BNAH (4.0×10^{-3} M) by HV^{2+} in the Presence of ZnP−C_{60} (3.0×10^{-6} M) or ZnP−H_2P−C_{60} (3.0×10^{-6} M) in Deoxygenated PhCN

catalyst	$[HV^{2+}]$/mM	Φ_{obs}
ZnP−C_{60}	2	0.65
	4	0.76
	8	0.87
	10	0.90
ZnP−H_2P−C_{60}	2	0.40
	8	0.40

SCHEME 3

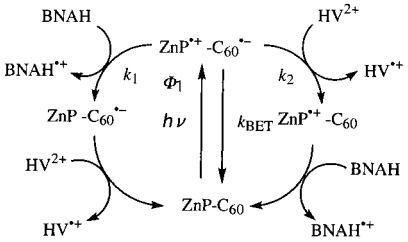

The quantum yields (Φ_{obs}) for the photochemical reaction of BNAH with HV^{2+} in the presence of ZnP−C_{60} or ZnP−H_2P−C_{60} were determined using a ferrioxalate actinometer[18] under irradiation with monochromatic light of $\lambda = 433$ nm. The Φ_{obs} value in the presence of ZnP−C_{60} (3.0×10^{-6} M) increases with increasing HV^{2+} concentration at a fixed BNAH concentration (4.0×10^{-3} M). Conversely, the Φ_{obs} value in ZnP−H_2P−C_{60} is invariant, irrespective of the chosen HV^{2+} concentration (Table 1). We ascribe this difference in concentration dependence to effects that evolve from the different lifetimes of radical ion pair in $ZnP^{\bullet+}-C_{60}^{\bullet-}$ and $ZnP^{\bullet+}-H_2P-C_{60}^{\bullet-}$ (vide infra).

BNAH is oxidized by the $ZnP^{\bullet+}$ moiety in the radical ion pair (k_1), whereas HV^{2+} is reduced by the $C_{60}^{\bullet-}$ moiety (k_2) as shown in Scheme 3. These individual electron transfer processes compete, however, with the BET in the radical ion pair (k_{BET}). $BNAH^{\bullet+}$ thus produced may disproportionate to give BNAH, BNA^+, and H^+,[23] when the overall redox reaction is given by eq 1.

By applying the steady-state approximation to the concentrations of the $ZnP^{\bullet+}$ and $C_{60}^{\bullet-}$ moieties in Scheme 3, the dependence of Φ_{obs} on [BNAH] and $[HV^{2+}]$ can be derived as given by eq 2

$$\Phi_{obs} = \frac{\Phi_1(k_1[\mathrm{BNAH}] + k_2[\mathrm{HV}^{2+}])}{k_{BET} + k_1[\mathrm{BNAH}] + k_2[\mathrm{HV}^{2+}]} \qquad (2)$$

where Φ_1 is the quantum yield of the radical ion pair formation. Under the experimental conditions (i.e., k_1[BNAH] or $k_2[HV^{2+}] \gg k_{BET}$), the limiting quantum yield (Φ_∞) corresponds to Φ_1. The dependence of Φ_{obs} on $[HV^{2+}]$ in the case of ZnP−C_{60} (Table 1) agrees with eq 2 from which the Φ_∞ value is determined as 0.99. This value agrees well with the Φ_1 value obtained independently from the direct kinetic analysis of the radical ion pair formation (0.99).[3] In the case of ZnP−H_2P−C_{60}, the Φ_∞ value agrees also with the Φ_1 value (0.40) obtained from the transient absorption spectrum.[3a] Such agreements confirm the validity of Scheme 3.

Equation 2 is reformulated to eq 3, which predicts, in principle, a linear correlation between $\Phi_{obs}/(\Phi_1 - \Phi_{obs})$ and $[HV^{2+}]$. With the help of Figure 4 this linear correlation was

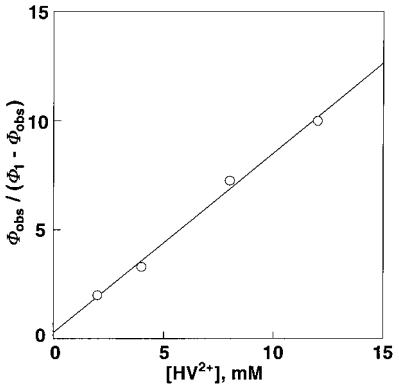

Figure 4. Plot of $\Phi_{obs}/(\Phi_1 - \Phi_{obs})$ vs $[HV^{2+}]$ for the photocatalytic oxidation of BNAH (4.0×10^{-4} M) by HV^{2+} with ZnP−C_{60} (3.0×10^{-6} M).

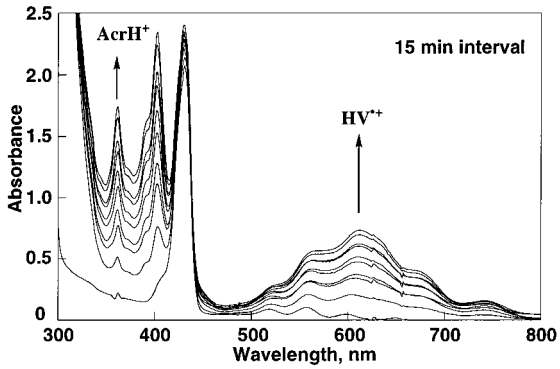

Figure 5. Spectral change observed in the steady-state photolysis of a PhCN solution of $AcrH_2$ (4.0×10^{-4} M), HV^{2+} (8.0×10^{-4} M), and ZnP−H_2P−C_{60} (3.0×10^{-6} M) under irradiation with monochromatized light of $\lambda = 433$ nm.

confirmed for the ZnP−C_{60} system. With k_{BET} (1.3×10^6 s^{-1}),[3] k_2 is derived from

$$\frac{\Phi_{obs}}{\Phi_1 - \Phi_{obs}} = \frac{k_2}{k_{BET}}[\mathrm{HV}^{2+}] + \frac{k_1[\mathrm{BNAH}]}{k_{BET}} \qquad (3)$$

the slope as $(1.0 \pm 0.1) \times 10^9$ M^{-1} s^{-1}.[24] This value agrees within experimental error with the value determined directly from the time-resolved experiment in Figure 2 [$(7\pm 2) \times 10^8$ M^{-1} s^{-1}].

Photocatalytic Oxidation of $AcrH_2$ by HV^{2+}. Upon replacing BNAH with $AcrH_2$ (4.0×10^{-3} M), photoinitiated ($\lambda =$ 433 nm) oxidation by HV^{2+} (8.0×10^{-3} M) produces $AcrH^+$ ($\lambda_{max} = 358$ nm) and $HV^{\bullet+}$ ($\lambda_{max} = 402$ and 615 nm) in the presence of ZnP−H_2P−C_{60}, as shown in Figure 5. The stoichiometry of the photocatalytic $AcrH_2$ oxidation (eq 4) is the same as established above for the BNAH oxidation (eq 1).

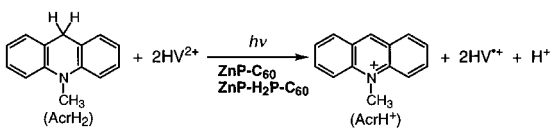

(4)

As is the case of the photocatalytic BNAH oxidation, the quantum yields were determined from an increase in absorbance due to $HV^{\bullet+}$ at 615 nm (Table 2). Hereby, the Φ values ($\Phi =$ 0.25 (ZnP−C_{60}) and 0.15 (ZnP−H_2P−C_{60})) are markedly reduced relative to the corresponding values obtained for the oxidation of BNAH ($\Phi = 0.87$ (ZnP−C_{60}) and 0.40 (ZnP−H_2P−C_{60})). We ascribe this decrease to the higher oxidation

TABLE 2: Quantum Yields (Φ_{obs}) of Photocatalytic Oxidation of $AcrH_2$ (4.0×10^{-3} M) by HV^{2+} (8.0×10^{-3} M) in the Presence of ZnP−C_{60} (3.0×10^{-6} M) or ZnP−H_2P−C_{60} (3.0×10^{-6} M) in the Absence and Presence of O_2 in PhCN

	Φ_{obs}	
catlyst	$O_2 = 0$ M	$O_2 = 8.5 \times 10^{-3}$ M
ZnP−C_{60}	0.25	0.02
ZnP−H_2P−C_{60}	0.15	0.14

potential of $AcrH_2$ (E^0_{ox} vs SCE = 0.81 V)[23] compared to that of BNAH (E^0_{ox} vs SCE = 0.57 V).[13] In this case, electron transfer from $AcrH_2$ to $ZnP^{\bullet+}$ is endergonic by 0.10 eV and, in turn, thermodynamically unfavorable. However, $AcrH_2^{\bullet+}$ is known to undergo a rapid deprotonation to produce subsequently $AcrH^{\bullet}$.[23] Following this deprotonation step, an electron transfer from $AcrH^{\bullet}$ to $ZnP^{\bullet+}$, forming $AcrH^+$, becomes now highly exergonic judging from the low oxidation potential of the $AcrH^{\bullet}$ species ($E^0_{ox} = -0.46$ V, which is equivalent to the one-electron reduction potential of $AcrH^+$).[25,26] Thus, the overall stoichiometry implies also a two-electron oxidation of $AcrH_2$ by two equivalents of HV^{2+} (eq 4), although the actual electron transfer event involving $AcrH_2$ is much slower than the corresponding oxidation of BNAH, leading consequently to the smaller quantum yields.

The amount of free energy (ΔG), stored in the photochemical oxidation of $AcrH_2$ by HV^{2+}, is obtained as 1.28 eV (124 kJ mol^{-1}) based on the difference between the redox potentials of the $AcrH_2/AcrH^+$ (0.22 V vs SCE)[26] and $HV^{2+}/HV^{\bullet+}$ (−0.42 V vs SCE) redox couples (eq 5). In the case of BNAH (E^0(BNAH/BNA^+) = 0.02 V),[27] the corresponding value is obtained as 0.88 eV (85 kJ mol^{-1}). In the dark, the back reaction

$$\Delta G = 2F[E^0(AcrH_2/AcrH^+)] - E^0(HV^{2+}/HV^{\bullet+}) \quad (5)$$

is extremely slow because of the kinetic barrier for a highly endergonic electron transfer from $HV^{\bullet+}$ ($E^0_{ox} = -0.42$ V vs SCE) to BNA^+ ($E^0_{red} = -1.08$ V vs SCE),[15] although the overall two-electron process is exergonic.[28,29]

Effects of O_2 on the Photocatalytic Systems. In the presence of oxygen, the lifetimes of both radical ion pairs (i.e., $ZnP^{\bullet+}$−$C_{60}^{\bullet-}$ and $ZnP^{\bullet+}$−H_2P−$C_{60}^{\bullet-}$) are reduced significantly because of an oxygen-catalyzed back electron transfer (BET) processes between $C_{60}^{\bullet-}$ and $ZnP^{\bullet+}$.[13] An intermolecular ET from $C_{60}^{\bullet-}$ to O_2 occurs via the coordination of O_2 to $ZnP^{\bullet+}$ to yield $O_2^{\bullet-}$ bound to $ZnP^{\bullet+}$, followed by a rapid intramolecular ET from $O_2^{\bullet-}$ to $ZnP^{\bullet+}$ in the $O_2^{\bullet-}$−$ZnP^{\bullet+}$ complex to regenerate O_2.[13] Such a binding of the radical anion to metal ion is known to accelerate the ET process.[30,31] The impact that such a reduction in lifetimes of the radical ion pairs has on the photocatalytic $AcrH_2$ oxidation was examined by deriving the quantum yield of formation of $AcrH^+$ from O_2-saturated PhCN solutions (see the Experimental Section).[32] The quantum yields under O_2-saturated conditions are also listed in Table 2.[33]

Surprisingly, the Φ_{obs} value (0.14) of the triad (ZnP−H_2P−C_{60}) system is little affected by molecular oxygen as compared to the value (0.15) found in the absence of O_2. In contrast to the triad, the Φ_{obs} value (0.02) of the dyad (ZnP−C_{60}) system becomes significantly smaller than the corresponding value (0.25) in the absence of O_2. It should be noted that the k_{BET} value of the triad increases from 4.8×10^4 s^{-1} to 3.2×10^5 s^{-1} in the absence and presence of O_2, respectively. This value is, however, still significantly smaller than the k_{BET} value of the dyad, even in the absence of O_2 (1.3×10^6 s^{-1}).[13] Furthermore, in the case of the triad (ZnP−H_2P−C_{60}), the rate of intermolecular electron transfer from $C_{60}^{\bullet-}$ to HV^{2+} (5.6×10^6 s^{-1} at 8.0×10^{-3} M HV^{2+}) is much faster than the BET rate (3.2×10^5 s^{-1}) in an O_2-saturated PhCN. This can be regarded as a potential rationale for the observation that the Φ_{obs} value of the triad (ZnP−H_2P−C_{60}) system is little affected by the presence of oxygen. Conversely, in the case of dyad (ZnP−C_{60}) the BET rate, especially in an O_2-saturated PhCN solution (1.5×10^7 s^{-1})[13] is much faster than the electron transfer rate, $C_{60}^{\bullet-}$ / HV^{2+}.

In conclusion, we have demonstrated that ZnP−linked−C_{60} systems act as efficient photocatalysts for the uphill oxidation of NADH analogues by HV^{2+}. The catalytic performance of the triad (ZnP−H_2P−C_{60}) system, which exhibits a much longer lifetime of the radical ion pair, is little affected by O_2, whereas the catalytic reactivity of the dyad (ZnP−C_{60}) is reduced significantly by the pure presence of O_2.

Acknowledgment. This work was supported by a grant-in-aid for Scientific Research Priority Area (No. 11228205) from the Ministry of Education, Science, Sports and Culture, Japan, the Sumitomo Foundation, and the Office of Basic Energy Sciences of the U.S. Department of Energy (contribution No. NDRL-4295 from the Notre Dame Radiation Laboratory).

References and Notes

(1) (a) Imahori, H.; Y. Sakata, Y. *Adv. Mater.* **1997**, *9*, 537. (b) Guldi, D. M. *Chem. Commun.* **2000**, 321. (c) Imahori, H.; Sakata, Y. *Eur. J. Org. Chem.* **1999**, 2445. (d) Fukuzumi, S.; Guldi, D. M. In *Electron Transfer in Chemistry*; Balzani, V., Ed.; Wiley-VCH: Weinheim, Germany, 2001; Vol. 2, pp 270−326.

(2) (a) Page, C. C.; Moser, C. C.; Chen, X.; Dutton, P. L. *Nature* **1999**, *402*, 47. (b) Gust, D.; Moore, T. A. In *The Porphyrin Handbook*; Kadish, K. M., Smith, K. M., Guilard, R., Eds.; Academic: San Diego, CA, 2000; Vol. 8, pp 153−190. (c) Gust, D.; Moore, T. A.; Moore, A. L. In *Electron Transfer in Chemistry*; Balzani, V., Ed.; Wiley-VCH: Weinheim, Germany, 2001; Vol. 3, pp 272−336.

(3) (a) Imahori, H.; Tamaki, K.; Guldi, D. M.; Luo, C.; Fujitsuka, M.; Ito, O.; Sakata, Y.; Fukuzumi, S. *J. Am. Chem. Soc.* **2001**, *123*, 2607. (b) Luo, C.; Guldi, D. M.; Imahori, H.; Tamaki, K.; Sakata, Y. *J. Am. Chem. Soc.* **2000**, *122*, 6535. (c) Imahori, H.; El-Khouly, M. E.; Fujitsuka, M.; Ito, O.; Sakata, Y.; Fukuzumi, S. *J. Phys. Chem. A* **2001**, *105*, 325.

(4) Fukuzumi, S.; Imahori, H. In *Electron Transfer in Chemistry*; Balzani, V., Ed.; Wiley-VCH: Weinheim, Germany, 2001; Vol. 2, pp 927−966.

(5) (a) Imahori, H.; Norieda, H.; Yamada, H.; Nishimura, Y.; Yamazaki, I.; Sakata, Y.; Fukuzumi, S. *J. Am. Chem. Soc.* **2001**, *123*, 100. (b) Imahori, H.; Yamada, H.; Ozawa, S.; Ushida, K.; Sakata, Y. *Chem. Commun.* **1999**, 1165. (c) Imahori, H.; Yamada, H.; Nishimura, Y.; Yamazaki, I.; Sakata, Y. *J. Phys. Chem. B* **2000**, *104*, 2099.

(6) (a) Vaidyalingam, A. S.; Coutant, M. A.; Dutta, P. K. In *Electron Transfer in Chemistry*; Balzani, V., Ed.; Wiley-VCH: Weinheim, Germany, 2001; Vol. 3, pp 412−486. (b) Borja, M.; Dutta, P. K. *Nature* **1993**, *362*, 43.

(7) (a) Hurst, J. K.; Khairutdinov. In *Electron Transfer in Chemistry*; Balzani, V., Ed.; Wiley-VCH: Weinheim, Germany, 2001; Vol. 3, pp 578−623. (b) Tabushi, I.; Kugimiya, S.; Mizutani, T. *J. Am. Chem. Soc.* **1983**, *105*, 1658. (c) Handman, J.; Harriman, A.; Porter, G. *Nature* **1984**, *307*, 534.

(8) (a) Steinberg-Yfrach, G.; Liddell, P. A.; Hung, S.-C.; Moore, A. L.; Gust, D.; Moore, T. A. *Nature* **1997**, *385*, 239. (b) Steinberg-Yfrach, G.; Rigaud, J.-L.; Durantini, E. N.; Moore, A. L.; Gust, D.; Moore, T. A. *Nature* **1998**, *392*, 479.

(9) Stryer, L. *Biochemistry*, 3rd ed.; Freeman: New York, 1988; Chapter 17.

(10) Fukuzumi, S. In *Advances in Electron Transfer Chemistry*; Mariano, P. S., Ed.; JAI Press: Greenwich, CT, 1992; pp 67−175.

(11) Fukuzumi, S.; Tanaka, T. *Photoinduced Electron Transfer*; Fox, M. A., Chanon, M., Eds.; Elsevier: Amsterdam, 1988; Part C, Chap. 10.

(12) Koper, N. W.; Jonker, S. A.; Verhoeven, J. W.; van Dijk, C. *Recl. Trav. Chim. Pays-Bas* **1985**, *104*, 296.

(13) Fukuzumi, S.; Imahori, H.; Yamada, H.; El-Khouly, M. E.; Fujitsuka, M.; Ito, O.; Guldi, D. M. *J. Am. Chem. Soc.* **2001**, *123*, 2571.

(14) Yamada, K.; Imahori, H.; Nishimura, Y.; Yamazaki, I.; Sakata, Y. *Chem. Lett.* **1999**, 895.

(15) Fukuzumi, S.; Koumitsu, S.; Hironaka, K.; Tanaka, T. *J. Am. Chem. Soc.* **1987**, *109*, 305.

(16) Roberts, R. M. G.; Ostovic, D.; Kreevoy, M. M. *Faraday Discuss. Chem. Soc.* **1982**, *74*, 257.

(17) Bruinink, J.; Kregting, C. G. A.; Ponjee, J. J. *J. Electrochem. Soc.* **1977**, *124*, 1854.

(18) Hatchard, C. G.; Parker, C. A. *Proc. R. Soc. London, Ser. A* **1956**, *235*, 518.

(19) Fukuzumi, S.; Nakanishi, I.; Suenobu, T.; Kadish, K. M. *J. Am. Chem. Soc.* **1999**, *121*, 3468.

(20) Fukuzumi, S.; Tokuda, Y.; Kitano, T.; Okamoto, T.; Otera, J. *J. Am. Chem. Soc.* **1993**, *115*, 8960.

(21) (a) Kadish, K. M.; Gao, X.; Van Caemelbecke, E.; Suenobu, T.; Fukuzumi, S. *J. Phys. Chem. A* **2000**, *104*, 3878. (b) Guldi, D. M.; Asmus, K.-D. *J. Phys. Chem. A* **1997**, *101*, 1472.

(22) The transient formation of $BNAH^{\bullet+}$ by electron transfer from BNAH to $ZnP^{\bullet+}$ was not examined because of the spectral overlap.

(23) Fukuzumi, S.; Kondo, Y.; Tanaka, T. *J. Chem. Soc., Perkin Trans. 2* **1984**, 673.

(24) The k_1 vlaue was determined from the intercept as $k_1 = 1.0 \times 10^9$ M^{-1} s^{-1}.

(25) Fukuzumi, S.; Ohkubo, K.; Tokuda, Y.; Suenobu, T. *J. Am. Chem. Soc.* **2000**, *122*, 4286.

(26) Hapiot, P.; Moiroux, J.; Savéant, J.-M. *J. Am. Chem. Soc.* **1990**, *112*, 1337.

(27) Anne, A.; Moiroux, J. *J. Org. Chem.* **1990**, *55*, 4608.

(28) An appropriate catalyst is thereby required to undergo the back reaction. As noted by Verhoeven et al.,[12] the energy stored in the photocatalytic reaction can, in principle, be made available via a photogalvanic device,[29] employing one electrode which specifically catalzyed the two-electron reduction of an NAD^+ analogue.

(29) Koper, N. W.; Verhoeven, J. W. *Proc. K. Ned. Akad. Wet., Ser. B* **1983**, *86*, 79.

(30) Fukuzumi, S.; Itoh, S. In *Advances in Photochemistry*; Neckers, D. C., Volman, D. H., von Bünau, G., Eds.; Wiley: New York, 1998; Vol. 25, pp 107−172.

(31) Fukuzumi, S. In *Electron Transfer in Chemistry*; Balzani, V., Ed.; Wiley-VCH: Weinheim, Germany, 2001; Vol. 4, pp 3−59.

(32) Because $HV^{\bullet+}$ is unstable in the presence of oxygen, the quantum yield was determined from increase in absorbance that is due to $AcrH^+$ at 358 nm.

(33) The O_2 concentrations in air- and O_2-saturated PhCN solutions were determined by the spectroscopic titration for the photooxidation of 10-methyl-9,10-dihydroacridine by O_2; see: Fukuzumi, S.; Ishikawa, M.; Tanaka, T. *J. Chem. Soc., Perkin Trans. 2* **1989**, 1037.